

## Turbulent Wall-Pressure Fluctuations in the CICLoPE Facility

Dacome, G.; Lazzarini, L.; Talamelli, A.; Bellani, G.; Baars, W. J.

**DOI**

[10.1007/978-3-031-55924-2\\_28](https://doi.org/10.1007/978-3-031-55924-2_28)

**Publication date**

2024

**Document Version**

Final published version

**Published in**

Progress in Turbulence 10 - Proceedings of the iTi Conference on Turbulence 2023

**Citation (APA)**

Dacome, G., Lazzarini, L., Talamelli, A., Bellani, G., & Baars, W. J. (2024). Turbulent Wall-Pressure Fluctuations in the CICLoPE Facility. In R. Örlü, R. Örlü, A. Talamelli, J. Peinke, & M. Oberlack (Eds.), *Progress in Turbulence 10 - Proceedings of the iTi Conference on Turbulence 2023* (pp. 213-219). (Springer Proceedings in Physics; Vol. 404 SPPHY). Springer. [https://doi.org/10.1007/978-3-031-55924-2\\_28](https://doi.org/10.1007/978-3-031-55924-2_28)

**Important note**

To cite this publication, please use the final published version (if applicable).  
Please check the document version above.

**Copyright**

Other than for strictly personal use, it is not permitted to download, forward or distribute the text or part of it, without the consent of the author(s) and/or copyright holder(s), unless the work is under an open content license such as Creative Commons.

**Takedown policy**

Please contact us and provide details if you believe this document breaches copyrights.  
We will remove access to the work immediately and investigate your claim.

***Green Open Access added to TU Delft Institutional Repository***

***'You share, we take care!' - Taverne project***

***<https://www.openaccess.nl/en/you-share-we-take-care>***

Otherwise as indicated in the copyright section: the publisher is the copyright holder of this work and the author uses the Dutch legislation to make this work public.

# Turbulent Wall-Pressure Fluctuations in the CICLoPE Facility



G. Dacome, L. Lazzarini, A. Talamelli, G. Bellani, and W. J. Baars

**Abstract** Wall-pressure spectra and coherence between wall-pressure and streamwise velocity in a turbulent pipe flow are presented. An experimental investigation was conducted in the CICLoPE long-pipe facility at friction Reynolds numbers in the range of  $4\,700 \lesssim Re_\tau \lesssim 46\,000$ . Wall-pressure energy spectra reveal an alignment of the inner-spectral peak location in terms of  $\lambda_x^+ \approx 250$ , as well as an increase in overall energy content with increasing  $Re_\tau$ . Linear coherence spectra between wall-pressure and streamwise velocity in the logarithmic region follow a Reynolds-number-independent wall-scaling. Identification of such a universal scaling contributes to compelling evidence that wall-pressure sensing, as an input for real-time flow control, is a feasible approach for implementation in practical engineering systems.

## 1 Introduction

Real-time control of large-scale structures in wall-bounded turbulent flows, for skin-friction drag reduction, requires a robust sensing architecture and scalability to application-level conditions. For Reynolds numbers of practical relevance, the friction Reynolds number  $Re_\tau \equiv \delta/l^* = \delta U_\tau/\nu$  (the ratio of inertial-to-viscous length scales) is in the order of  $\mathcal{O}(10^3)$  to  $\mathcal{O}(10^6)$ . Here,  $\delta$  is the boundary layer thickness (in our work equal to the pipe radius  $R$ ),  $U_\tau \equiv \sqrt{\tau_w/\rho}$  is the friction velocity (with  $\tau_w$  being the wall-shear stress and  $\rho$  the fluid density) and  $\nu$  is the kinematic viscosity. At these conditions, large-scale motions in the logarithmic region become (1) energetically dominant over the near-wall structures, and (2) the primary contributor to the bulk turbulence kinetic energy production. And so, large-scale turbulence forms

---

G. Dacome (✉) · W. J. Baars

Faculty of Aerospace Engineering, Delft University of Technology, 2629HS  
Delft, The Netherlands  
e-mail: [g.dacome@tudelft.nl](mailto:g.dacome@tudelft.nl)

L. Lazzarini · A. Talamelli · G. Bellani

Dipartimento di Ingegneria Industriale, Università di Bologna, 47121 Forlì, Italy

© The Author(s), under exclusive license to Springer Nature Switzerland AG 2024  
R. Örlü et al. (eds.), *Progress in Turbulence X*, Springer Proceedings in Physics 404,  
[https://doi.org/10.1007/978-3-031-55924-2\\_28](https://doi.org/10.1007/978-3-031-55924-2_28)

213

an attractive target for streamwise-persistent control [1]. Given the requirement to minimize form drag, the question arises as to whether wall-pressure (which is a relatively easy quantity to measure) can serve as an input for detecting large-scale velocity fluctuations.

Studies of the wall-pressure in turbulent wall-bounded flows have been carried out by means of both numerical and wind tunnel experiments. Literature (e.g. Farabee and Casarella [2] and Klewicki et al. [3] for experimental work, and Panton et al. [4] for a numerical study) reports the Reynolds-number scaling of wall-pressure energy spectra and its intensity. An inner-spectral peak was found to reside around a streamwise wavelength of  $\lambda_x^+ \equiv \lambda_x U_\tau / \nu \approx 250$ . Its peak-magnitude increases as a function of  $Re_\tau$  and so does the large-scale energy content. Relations between wall-pressure events and turbulent velocities have also been investigated. For instance, Thomas and Bull [5] revealed characteristic wall-pressure signatures associated with near-wall burst-sweep events. Spatio-temporal correlation between streamwise velocity and wall-pressure have also been studied [6]. These have revealed a low but significant coherence between the low-frequency content of the wall-pressure signal and the velocity in the logarithmic region of a Turbulent Boundary Layer (TBL) caused by the passage of large-scale motions.

With the goal of analysing the potential of wall-pressure as an input to real-time control for skin-friction drag reduction in wall-bounded turbulence, we present an experimental investigation of the Reynolds-number scaling of the wall-pressure spectrum in high-Reynolds-number pipe flow. Additionally, we investigate the scaling of the scale-dependent correlation between wall-pressure and streamwise velocity in the logarithmic region. This will provide insight into whether wall-pressure can be employed as a wall-based input for real-time control when considering both laboratory- and application-level Reynolds numbers.

## 2 Experimental Methodology

Experiments were carried out in the Centre for International Cooperation in Long-Pipe Experiments (CICLoPE, see Fig. 1a, b). The facility comprises a 111.15 m-long circular pipe with a radius of  $R = 0.4505$  m; for the reported experiments the friction Reynolds number was in the range  $4\,700 \lesssim Re_\tau \lesssim 46\,000$ . All testing conditions considered are reported in Table 1. The flow in the test section (at the downstream end of the pipe) can be considered fully developed. Additional information on the design of the facility can be found in the work of Bellani and Talamelli [7].

Pressure sensors were integrated in the wall of the pipe within a cavity communicating with the flow by means of a pinhole orifice, having a diameter of  $d_p = 0.3$  mm. The resonance frequency of the cavity was found via an acoustic characterization experiment, whereby inlet and cavity pressures were measured simultaneously in quiescent flow and correlated in the frequency domain. A second-order model was fit to the gain of the linear transfer function,  $|H_p|$ , relating inlet to cavity pressure [8]. Figure 1c presents the gain curve and shows resonance at  $f_r \approx 4$  kHz.

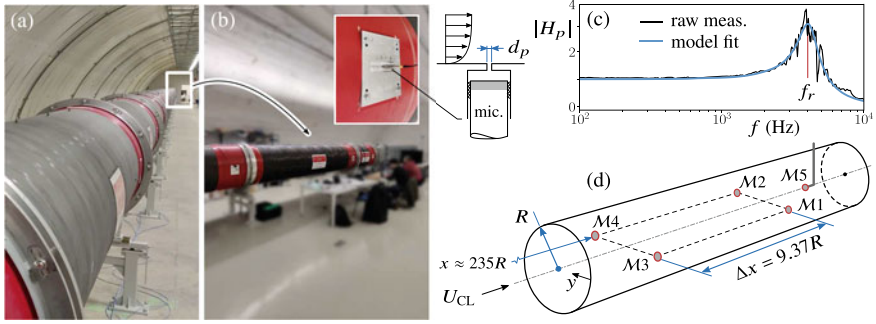


**Fig. 1** **a, b** Photographs of the CICLoPE facility and test section; **b** one of the four wall plugs with the microphone sensor; **c** gain of the transfer function between inlet and cavity pressures, measured in quiescent flow; **d** microphone lay-out with  $x = 0$  corresponding to the pipe inlet

Time-resolved pressure sensing was performed using GRAS 46BE 1/4-in. CCP free-field microphones. Their dynamic range is 35–160 dB and their accuracy is  $\pm 1$  dB in the range of 10 Hz to 40 kHz. Each measurement was performed with an acquisition frequency of  $f_s = 51.2$  kHz and with a 24-bit A/D conversion for an uninterrupted duration of  $T_a = 240$  s. Five microphones were employed in our study (labelled  $\mathcal{M}1$  to  $\mathcal{M}5$  in Fig. 1d): four were integrated in the wall of the pipe ( $\mathcal{M}1$  to  $\mathcal{M}4$ ) for wall-pressure measurements and one was mounted along the pipe's centreline ( $\mathcal{M}5$ ) for monitoring the acoustic noise of the facility. The wall-mounted microphones were arranged in two streamwise pairs, separated by a distance of 4.22 m ( $\Delta x = 9.37R$ ). Microphones in one pair were located in azimuthally-opposite positions on the pipe wall to facilitate noise-filtering in post-processing.

Time series of streamwise velocity at a fixed wall-normal location in the logarithmic region ( $y_{HW} = 0.011$  m) were acquired using Hot-Wire Anemometry (HWA), simultaneously with all pressure signals. A Dantec Streamline 90C10 CTA module was used, with a standard Dantec 55P15 boundary layer probe.

### 3 Wall-Pressure Filtering and Scaling

Before analysing the hydrodynamic wall-pressure signal and, in particular, its energy spectrum  $\phi_{pp}$ , the effects of cavity resonance as well as facility acoustic noise must be removed. The correction for cavity resonance is applied directly in the frequency domain following  $\phi_{pp} = \tilde{\phi}_{pp}/|H_p|^2$  (with  $\tilde{\phi}_{pp}$  being the spectrum of the raw pressure time series). The result of this correction is reported in Fig. 2a, where the raw wall-pressure spectra are displayed as a function of streamwise wavelength,  $\lambda_x^+ \equiv U_c^+/f^+$  ( $U_c^+ = 10$  is the convection velocity and  $f^+$  the frequency, both inner-scaled). For the three highest Reynolds number data sets 5 to 7, a wiggle in the spectrum appears around the location of the inner-spectral peak at  $\lambda_x^+ \approx 250$ . This wiggle is ascribed

**Table 1** Test conditions in the CICLoPE long-pipe facility. Superscript ‘+’ indicates inner-scaling

Data set	Pipe flow conditions					Sensor parameters						
	Colour	$Re_{\tau}$	$\tau_w$ (Pa)	$U_{\tau}$ (m/s)	$l^*$ ( $\mu\text{m}$ )	$U_{CL}$ (m/s)	$d_p^+$	$l_{HW}^+$	$y_{HW}^+$	$f_s^+$	$T_a U_{CL}/R$	
1	—	4797	0.031	0.161	93.8	3.837	3.17	13.2	116	4.84	2036	
2	—	7079	0.068	0.238	63.6	5.833	4.68	19.5	172	3.28	3129	
3	—	13647	0.265	0.470	32.3	12.11	9.23	38.4	338	1.67	6487	
4	—	22789	0.710	0.769	19.7	20.71	15.1	62.9	553	1.02	11079	
5	—	31439	1.358	1.065	14.3	29.50	20.9	87.0	766	0.74	15792	
6	—	37966	1.983	1.287	11.9	36.13	25.3	105	927	0.61	19325	
7	—	45810	2.902	1.559	98.2	44.60	31.0	129	1138	0.50	24081	

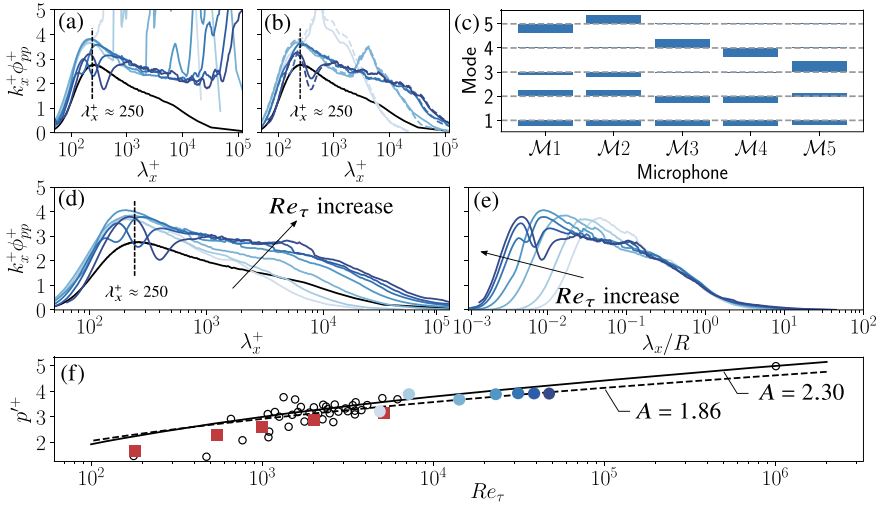


**Fig. 2** **a** Wall-pressure spectra prior to application of noise removal procedures but with Helmholtz resonance correction applied; **b** noise-corrected spectra with LSE- (solid) and Wiener filtering-procedures (dashed); **c** spatial POD mode shapes of the pressure signals; **d**, **e** noise-corrected spectra with POD technique as a function of inner- and outer-scaled wavelength; **f** wall-pressure intensity taken as the integral of the spectra (filled blue markers), compared to literature data (hollow markers) including the DNS data by Panton et al. [4] (filled red markers) and empirical relations reported by Klewicki et al. [3] (solid and dashed curves)

to an imperfect correction for cavity resonance: the presence of the flow slightly alters the resonance frequency of the pinhole cavity in comparison to the acoustic calibration experiment. Note that at low Reynolds numbers the resonance frequency is far beyond the energetic frequency range of the wall-pressure spectrum.

Facility noise removal is a crucial pre-processing step [9] and three different strategies were attempted. The first two procedures rely on the estimation of a correction time series  $\tilde{p}(t)$  from a single microphone pair ( $\mathcal{M}1$  and  $\mathcal{M}2$ ), which is subtracted from the raw signal (here  $\mathcal{M}1$ ) to obtain the noise-corrected wall-pressure signal,  $p_w(t) = p_1(t) - \tilde{p}(t)$ , with  $p_1(t)$  being the raw pressure time series. Both Linear Stochastic Estimation (LSE) and an adaptive Wiener filtering approach were applied to generate  $\tilde{p}(t)$  and yielded similar results, displayed in Fig. 2b. For the low Reynolds-number data sets an unexpected hump is still present in the range  $300 < \lambda_x^+ < 10^4$ .

A third and most effective noise removal approach implemented is based on Proper Orthogonal Decomposition (POD). This method is superior in performance with respect to the other methods both in virtue of its lower overhead and the fact that it employs signals from all five microphones. First, all time series are temporally aligned to compensate for excessive lags in the cross-correlation. Following a conventional POD implementation [10], the five spatial modes are shown in Fig. 2c. After conducting an analysis on the coupling of POD modes, through scrutinizing the

correlation of the (temporal) expansion coefficients, it was concluded that only the 4th and 5th modes capture the pressure fluctuations that are incoherent between sensors. As such, noise-corrected wall-pressure signals are reconstructed by considering these two modes only and the resulting spectra are reported in Fig. 2d. Alignment of the inner-spectral peak at  $\lambda_x^+ \approx 250$  is observed, as well as a progressive increase in large-scale energy content with increasing  $Re_\tau$ , in accordance with literature. Additionally, the large-scale tails of the spectra collapse when the streamwise wavelength is scaled in outer units (Fig. 2e). Finally, validation of the noise-removal approach is provided by comparing the wall-pressure intensity to empirical relations [3]: Fig. 2f shows good agreement between the intensity inferred from integrating the spectra after POD-filtering and the findings of the literature.

## 4 Wall-Pressure–Velocity Coupling

The linear coherence spectrum  $\gamma_{up_w}^2$  is employed to describe the correlation between streamwise velocity in the logarithmic region and wall-pressure. Baars et al. [11] report an analysis of this coherence for a relatively low Reynolds number range up to  $Re_\tau \approx 5\,200$ . A comparison between  $\gamma_{up_w}^2$  extracted from Direct Numerical Simulation (DNS) data [12] and experiments [11] is displayed in Fig. 3a for  $Re_\tau \approx 2\,000$ . Here, the spectral coherence is plotted versus the distance-from-the-wall-scaled streamwise wavelength. Curves are shown for several wall-normal locations within the logarithmic region. The broadband hump centered at  $\lambda_x/y \approx 14$  reasonably collapses, with a maximum at  $\gamma_{up_w}^2 \approx 0.1$ .

An identical analysis applied to the high-Reynolds-number CICLoPE data results in the spectra shown in Fig. 3b. Coherence spectra reveal a trend similar to the lower- $Re_\tau$  data in Fig. 3a, and also peak near  $\lambda_x/y \approx 14$ . Despite the relatively low value in coherence, results suggest Reynolds-number-independent wall-scaling. These scaling results, together with an in-depth analysis of wall-pressure-based

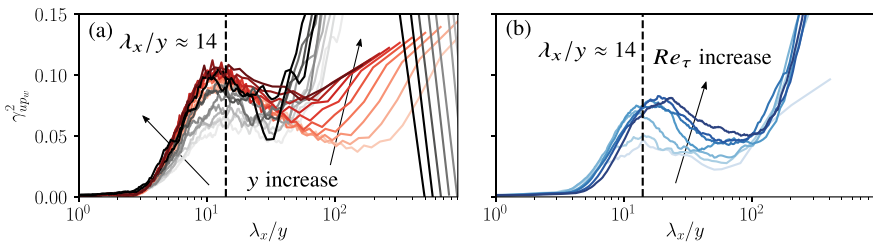


**Fig. 3** **a** Coherence spectra of wall-pressure and streamwise velocity in the logarithmic region for DNS channel flow data (red, [12]) and experimental data (black, [11]) at  $Re_\tau \approx 2\,000$  and for 10 logarithmically spaced locations in the range  $y^+ \in (80, 200)$ . **b** Coherence spectra of wall-pressure and velocity for data acquired in the CICLoPE facility



velocity-estimation [11], illustrate how wall-pressure sensing for real-time flow control is viable at high-Reynolds-number conditions.

## 5 Concluding Remarks

Upon removing facility noise from the wall-pressure time series, by means of a multi-sensor POD-based approach, energy spectra of wall-pressure fluctuations reveal good alignment of the small-scale energy peak at  $\lambda_x^+ \approx 250$ , as well as an expected increase in large-scale energy content with increasing Reynolds number. The intensity of the noise-corrected wall-pressure signals also agrees with empirical relations derived in the literature, further validating the noise-removal approach. Coherence spectra of wall-pressure and velocity further proved a Reynolds-number-independent wall-scaling, which is encouraging when considering wall-pressure for real-time control in practical engineering systems.

**Acknowledgements** The work of the UniBo team was carried out within the MOST—Sustainable Mobility National Research Center and received funding from the European Union Next-Generation EU (PIANO NAZIONALE DI RIPRESA E RESILIENZA (PNRR)—MISSIONE 4 COMPONENTE 2, INVESTIMENTO 1.4—D.D. 1033 17/06/2022, CN00000023).

## References

1. N. Renard, S. Deck, A theoretical decomposition of mean skin friction generation into physical phenomena across the boundary layer. *J. Fluid Mech.* **790**, 339–367 (2016)
2. T.M. Farabee, M.J. Casarella, Spectral features of wall pressure fluctuations beneath turbulent boundary layers. *Phys. Fluids A* **3**(10), 2410–2420 (1991)
3. J.C. Klewicki, P.J.A. Priyadarshana, M.M. Metzger, Statistical structure of the fluctuating wall pressure and its in-plane gradients at high Reynolds number. *J. Fluid Mech.* **609**, 195–220 (2008)
4. R.L. Panton, M. Lee, R.D. Moser, Correlation of pressure fluctuations in turbulent wall layers. *Phys. Rev. Fluids* **2**(9), 094604 (2017)
5. A.S.W. Thomas, M.K. Bull, On the role of wall-pressure fluctuations in deterministic motions in the turbulent boundary layer. *J. Fluid Mech.* **128**, 283–322 (1983)
6. B. Gibeau, S. Ghaemi, Low- and mid-frequency wall-pressure sources in a turbulent boundary layer. *J. Fluid Mech.* **918**, A18 (2021)
7. G. Bellani, A. Talamelli, The final design of the long pipe in CICLoPE, in *Progress in Turbulence VI* (2016), pp. 205–209
8. Y. Tsuji, J.H.M. Fransson, P.H. Alfredsson, A.V. Johansson, Pressure statistics and their scaling in high-Reynolds-number turbulent boundary layers. *J. Fluid Mech.* **585**, 1–40 (2007)
9. A.M. Naguib, S.P. Gravante, C.E. Wark, Extraction of turbulent wall-pressure time-series using an optimal filtering scheme. *Exp. Fluids* **22**, 14–22 (1996)
10. C.E. Tinney, P. Jordan, The near pressure field of co-axial subsonic jets. *J. Fluid Mech.* **611**, 175–204 (2008)
11. W.J. Baars, G. Dacome, M. Lee, Reynolds-number scaling of wall-pressure–velocity correlations in wall-bounded turbulence. *J. Fluid Mech.* **981**, A15 (2024)
12. M. Lee, R.D. Moser, Direct numerical simulation of turbulent channel flow up to  $Re_\tau = 5200$ . *J. Fluid Mech.* **774**, 395–415 (2015)